Inverted-V chirped phased arrays of gain-guided GaAs/GaAlAs diode lasers

E. Kapon, C. P. Lindsey, J. S. Smith, S. Margalit, and A. Yariv
California Institute of Technology, Pasadena, California 91125

(Received 24 August 1984; accepted for publication 24 September 1984)

Inverted-V chirped arrays of multiple quantum well GaAs/GaAlAs lasers were grown by molecular beam epitaxy. These arrays consisted of seven gain-guided lasers whose stripe widths decreased, from the central laser to the outermost ones, symmetrically. This structure makes it possible to discriminate against the higher order array supermodes, which results in diffraction limited beams with a single lobe directed perpendicular to the laser facet. Single lobed far-field patterns, 3°–4° wide, were obtained from inverted-V chirped arrays operated up to $1.5I_{th}$. The supermode structure of these arrays was identified by studying their spectrally resolved near fields.

Phase-locked arrays of diode lasers can produce single lobed, diffraction limited beams directed normal to the laser facet only if they oscillate in the fundamental array supermode.[1,2] However, most phased arrays demonstrated thus far exhibited double lobed beams,[3–5] because of their tendency to oscillate in the higher order supermodes.[1,2] Recently, we have shown theoretically that by employing certain nonuniform array structures, it is possible to achieve efficient discrimination against all the higher order supermodes.[6,7] More specifically, by varying the widths of the laser waveguides and, in addition, creating a proper gain distribution across the array, one can select the fundamental array supermode. Single lobed, diffraction limited beams (though deflected from the facet normal) were indeed obtained from linearly chirped gain-guided arrays of GaAs/GaAlAs lasers grown by liquid phase epitaxy (LPE).[8] In the present letter we report on the performance of symmetric, inverted-V chirped arrays of gain-guided GaAs/GaAlAs lasers grown by molecular beam epitaxy (MBE). These symmetrically chirped arrays can oscillate in the fundamental supermode and, therefore, emit diffraction limited, single lobed beams that are directed normal to the array facet. The use of MBE grown wafers in these nonuniform array structures is particularly effective because of the wafer uniformity. This uniformity makes it possible to produce the desired variation in the propagation constants of the array channels[6,7] in a controlled fashion.

The schematic cross section of the inverted-V chirped array is shown in Fig. 1. The arrays were fabricated from MBE grown multiple quantum well GaAs/GaAlAs wafers. The following layer structure was grown on an n^+-GaAs substrate: 1.5-μm Sn-doped $Ga_{0.7}Al_{0.3}As$, $n \simeq 2\times10^{17}$ cm^{-3} (cladding layer); four GaAs quantum wells, 200 Å each, spaced by three 220-Å $Ga_{0.9}Al_{0.1}As$ barriers (active region); 2-μm Be-doped $Ga_{0.7}Al_{0.3}As$, $p \simeq 2\times10^{17}$ cm^{-3} (cladding layer); and 0.2-μm Be-doped GaAs, $p \simeq 2\times10^{18}$ cm^{-3} (contact layer). The seven laser stripes in each array were defined by shallow proton implantation (80-keV protons, 3×10^{15} cm^{-2} dose) through a photoresist mask. The implanted regions penetrated down to about 0.7 μm from the surface of the wafer. The widths of the laser stripes varied from 7 μm at the central channel to 4 μm at the outermost channels, symmetrically, in steps of 1 μm. The channel spacing was 2 μm. A single Cr/Au contact layer was used on the p side of the array, and AuGe/Au contact was used on the n side.

The variation in the widths of the channels in the chirped array results in a variation of the (complex) propagation constant β of the guided optical mode in each channel. This variation in β, in turn, modifies the near-field patterns of the array supermodes, compared to those in a uniform array. In the inverted-V chirped array, the power of the fundamental supermode is concentrated in the central channels, whereas the higher order supermodes are more localized in the outermost channels.[6,7] Since the gain in the active region is larger under the wider laser stripes,[9] the fundamental supermode is expected to have higher modal gain (near threshold). This combination of modal power redistribution, compared to uniform arrays, and profiled gain results in the preferred fundamental supermode oscillation.

A basic optical model was developed for the inverted-V chirped array. Following the effective index method,[10] the y component of the electric field can be written as $E_y(x,y,z,) = F(x,y)\mathscr{E}(y)\exp(i\beta z)$, where β is the propagation constant and F depends weakly on y (see Fig. 1 for definition of the coordinate system). For the case of weakly coupled channels, we may write

$$\mathscr{E}(y) = \bar{\mathscr{E}}(y)\sum_{l=1}^{N}\mathscr{E}_l(y-y_l), \tag{1}$$

where $\bar{\mathscr{E}}(y)$ is a slowly varying envelope function and $\mathscr{E}_l(y)$, $l = 1,2,\cdots N$, describe the lateral field distributions in each of the N individual channels which are centered about $y = y_l$. It can be shown[7] that $\bar{\mathscr{E}}$ satisfies approximately the Helm-

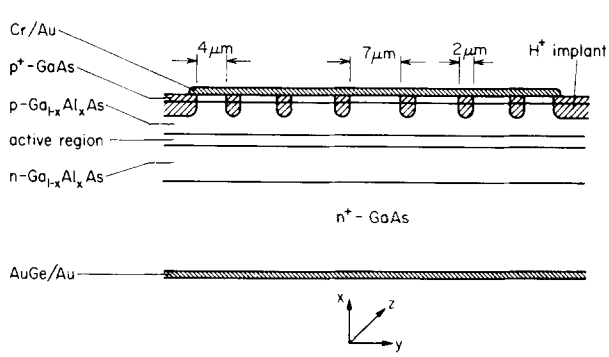

FIG. 1. Schematic cross section of the inverted-V chirped array.

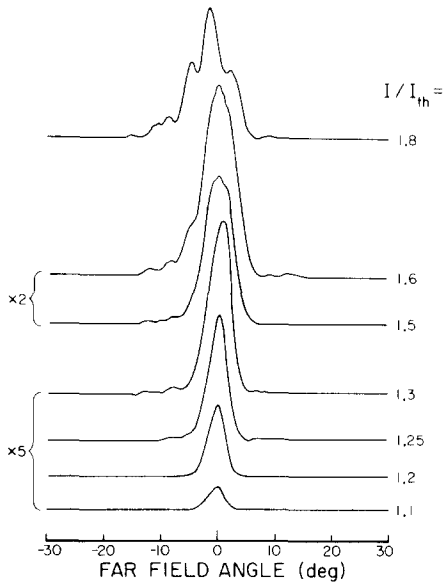

FIG. 2. Far-field patterns (in the junction plane) of an inverted-V chirped array for various array currents. The threshold current was $I_{th} = 250$ mA.

holtz equation

$$d^2\bar{\mathscr{E}}/dy^2 + [k_o^2\bar{\epsilon}(y) - \beta^2]\bar{\mathscr{E}} = 0, \tag{2}$$

where $\bar{\epsilon}(y)$ is a smooth function for which $\bar{\epsilon}(y_l) = \beta_l^2/k_o^2$, β_l being the propagation constant in the l th channel. ($k_o = 2\pi/\lambda_o$, where λ_o is the free-space wavelength.) Approximating $\bar{\epsilon}(y)$ by a parabolic distribution,

$$\bar{\epsilon}(y) = \bar{\epsilon}(0) - (P/k_o^2)y^2 \tag{3}$$

the solution of (2) is

$$\bar{\mathscr{E}}_\nu(y) = H_\nu(P^{1/4}y)\exp(-P^{1/2}y^2/2), \tag{4a}$$

$$\beta^2 = k_o^2\bar{\epsilon}(0) - (2\nu + 1)P^{1/2} \qquad \nu = 1,2,\cdots N, \tag{4b}$$

where H_ν are Hermite polynomials. If the field distributions $\mathscr{E}_l$ do not change much with l, one can approximate the far-field patterns of the supermodes by

$$\tilde{\mathscr{E}}_\nu(\theta) \propto \tilde{\mathscr{E}}_l(\theta)H_\nu[k_o \sin\theta/P^{1/4}]$$
$$\times\exp[-(k_o \sin\theta)^2/(2P^{1/2})], \tag{5}$$

where θ is the far-field angle (in the junction plane) and $\tilde{\mathscr{E}}_l(\theta)$ is the far-field distribution of each individual array element. Equations (4) and (5) show that, for an inverted-V chirped array, the envelopes of the supermode near fields and the supermode far-field patterns can be approximated by Gauss–Hermite functions.

The inverted-V chirped arrays were tested under low duty cycle pulsed conditions (200-ns pulses). The threshold current was typically 200 mA for 250-μm-long devices. Figure 2 shows the evolution of the far-field pattern (measured parallel to the junction plane) of such an array as the pumping level is increased. The far-field pattern consisted of a single lobed pattern up to more than $1.5I_{th}$. The beam full width at half-maximum power (FWHP) increased from less than 3° at $1.1I_{th}$ to about 4° at $1.5I_{th}$. A remarkable property of the beam shape (at these pump levels) is that virtually all the beam power is contained within the main lobe, unlike the situation in other "single lobed" radiation patterns described previously.[11–13] This single lobed pattern is consistent with the Gaussian far-field pattern of the fundamental supermode predicted by Eq. (5). At higher excitation levels

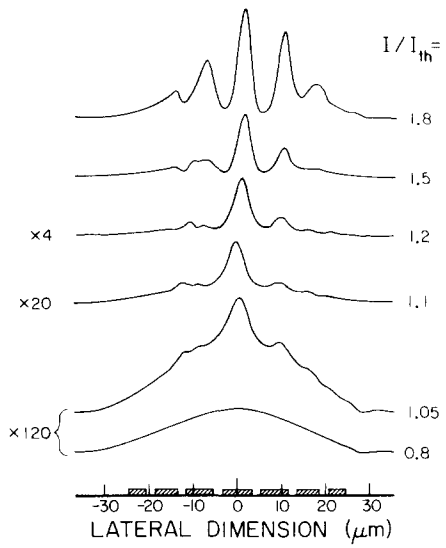

FIG. 3. Near-field patterns (in the junction plane of an inverted-V chirped array for various array currents. The threshold current was $I_{th} = 250$ mA. The cross-hatched regions indicate the location of the laser stripes.

the beam divergence increased and additional structure appeared beside the main lobe (see Fig. 2). This is due to the excitation of higher order supermodes as discussed below.

The evolution of the near-field pattern (in the junction plane) at increasing pump levels is shown in Fig. 3. Below threshold, the spontaneous emission distribution mimicks, approximately, the gain distribution across the array (at

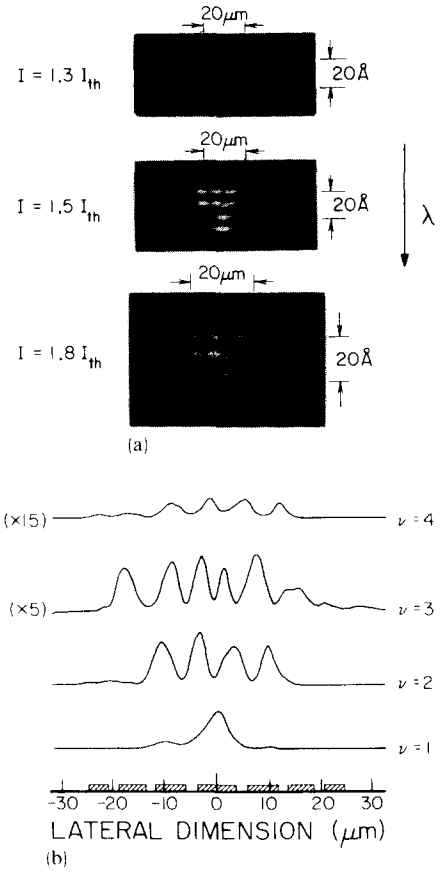

FIG. 4. (a) Spectrally resolved near-field photographs of an inverted-V chirped array, at various array currents. The wavelength is 0.87 μm. (b) Near-field patterns of the four resolved supermodes observed at $I = 1.8I_{th}$. The cross-hatched regions indicate the location of the laser stripes.

threshold), and demonstrates how the stripe design serves to tailor the lateral gain distribution so as to favor the fundamental supermode. Up to about $1.5I_{th}$, the near-field intensity is localized in the central array channels. Assuming a Gaussian far-field pattern with FWHP of 3°, Eqs. (4) and (5) imply that the *envelope* of the near-field pattern be a Gaussian with FWHP of 7.6 μm ($\lambda = 0.9$ μm was used). This is consistent with the patterns in Fig. 3. In this sense, the far-field patterns of Fig. 2 (close to threshold) are diffraction limited. At currents above $1.5I_{th}$, more power is seen to appear in the outermost array channels. This is due to the excitation of higher order supermodes and is consistent with the far-field broadening shown in Fig. 2.

Figure 4(a) shows photographs of the spectrally resolved near field of the chirped array, obtained at various currents above threshold. Closer to the threshold, the array lased in essentially a single longitudinal mode as well as in the fundamental supermode. At higher currents additional supermodes could be identified in the spectrally resolved near field, as was deduced from their different spatial intensity patterns and from their different frequencies. At $I = 1.8I_{th}$, four supermodes could be observed clustered about the Fabry–Perot (FP) mode frequencies. Their measured spatial intensity distributions are shown in Fig. 4(b). These supermode patterns have the general feature that the lowest order ones are more localized in the array center, as expected from the Gauss–Hermite approximate solutions in (4). At least for the lowest order supermodes $\nu = 1$ and $\nu = 2$, one can identify near-field envelopes which agree qualitatively with those predicted by (4a). Note that the higher order supermodes appear at *shorter* wavelengths, in agreement with (4b). The splitting between the supermode frequencies, in units of the FP mode spacing, is 0.2 betwen $\nu = 1$ and $\nu = 2$ and 0.1 between $\nu = 2$ and $\nu = 3$ or $\nu = 3$ and $\nu = 4$. Using the value of 3° for the FWHP of the fundamental supermode far field, $\lambda_0 = 0.87$ μm, the effective mode index equals to 3.4, and the measured diode length $L = 150$ μm, Eq. (4b) gives a constant frequency splitting of 0.1 times the FP mode spacing. A better fit to the experimental data is obtained using a sech^2 profile for the gain distribution, instead of (3).

In the chirped arrays, the discrimination against the higher order supermodes is achieved due to the larger overlap of the near-field pattern of the fundamental supermode with the gain distribution. However, this discrimination is maintained only at sufficiently low power levels at which gain saturation effects are not important. At higher power levels, the gain distribution becomes depleted in the array center due to stimulated emission into the fundamental supermode. This spatial hole burning results in the excitation of the higher order supermodes, as was observed in the experimental results described above. The pump level at which the higher order supermodes dominate depends on the photon density in the fundamental supermode which, in turn, depends on the rate at which the envelope of the effective dielectric constant $\bar{\epsilon}(y)$ [see (2)] changes across the array. Clearly, a more moderate variation of $\bar{\epsilon}$ can postpone the appearance of the higher order supermodes to higher power levels and would also reduce the beam divergence of the fundamental supermode. This can be achieved, e.g., by using a more moderate variation in the stripe widths. On the other hand, a too small variation in $\bar{\epsilon}(y)$ would reduce the supermode discrimination at threshold [as obviously happens in the limit of constant $\bar{\epsilon}(y)$, i.e., in the case of a uniform array[6]]. Thus, the single contact chirped arrays should be properly designed in order to achieve optimal performance. One possible way to avoid the appearance of the higher order supermodes is to use separate laser contacts[14] in order to modify the gain distribution across the array at each power level, as to maintain a fundamental supermode operation.

The research described in this paper was performed under contracts with the U.S. Office of Naval Research and the National Science Foundation. E. Kapon acknowledges the support of a Weizmann Postdoctoral Fellowship. J. S. Smith gratefully acknowledges the support of the Fannie and John Hertz Foundation. We thank Dr. M. Nicolet and Mr. Ali Ghaffari for the proton implantation.

[1] E. Kapon, J. Katz, and A. Yariv, Opt. Lett. **9,** 125 (1984).
[2] J. K. Butler, D. E. Ackley, and D. Botez, Appl. Phys. Lett. **44,** 293 (1984).
[3] D. R. Scifres, W. Streifer, and R. D. Burnham, Appl. Phys. Lett. **33,** 616 (1978).
[4] D. R. Scifres, R. D. Burnham, and W. Streifer, Appl. Phys. Lett. **41,** 118 (1982).
[5] H. Temkin, R. D. Dupuis, R. A. Logan, and T. P. van der Ziel, Appl. Phys. Lett. **44,** 473 (1984).
[6] E. Kapon, C. P. Lindsey, J.Katz, S. Margalit, and A. Yariv, Appl. Phys. Lett. **45,** 200 (1984).
[7] E. Kapon and A. Yariv (unpublished)
[8] C. P. Lindsey, E. Kapon, J. Katz, S. Margalit, and A. Yariv, Appl. Phys. Lett. **45,** 722 (1984).
[9] G. H. B. Thompson, *Physics of Semiconductor Laser Devices* (Wiley, New York, 1980), p. 346.
[10] W. Streifer and E. Kapon, Appl. Opt. **18,** 3724 (1979) and references therein.
[11] D. R. Scifres, R. D. Burnham, and W. Streifer, Appl. Phys. Lett. **41,** 614 (1982).
[12] J. Katz, S. Margalit, and A. Yariv, Appl. Phys. Lett. **42,** 554 (1983).
[13] D. Botez and T. C. Connolly, Appl. Phys. Lett. **43,** 1096 (1983).
[14] J. Katz, E. Kapon, C. Lindsey, U. Shreter, S. Margalit, and A. Yariv, Appl. Phys. Lett. **43,** 521 (1983).